

Electronic structure and bonding in garnet crystals $\text{Gd}_3\text{Sc}_2\text{Ga}_3\text{O}_{12}$, $\text{Gd}_3\text{Sc}_2\text{Al}_3\text{O}_{12}$, and $\text{Gd}_3\text{Ga}_3\text{O}_{12}$ compared to $\text{Y}_3\text{Al}_5\text{O}_{12}$

Yong-Nian Xu and W. Y. Ching*

Department of Physics, University of Missouri-Kansas City, Kansas City, Missouri 64110

B. K. Briceken

Allied Signal FM & T, Kansas City, Missouri 64141

(Received 16 July 1999)

The electronic structure and bonding of $\text{Gd}_3\text{Sc}_2\text{Ga}_3\text{O}_{12}$ (GSGG), $\text{Gd}_3\text{Sc}_2\text{Al}_3\text{O}_{12}$ (GSAG), and $\text{Gd}_3\text{Ga}_3\text{O}_{12}$ (GGG) crystals with a garnet structure are studied by means of first-principles local-density calculations. The results are compared with a similar calculation on yttrium aluminum garnet [$\text{Y}_3\text{Al}_5\text{O}_{12}$ (YAG)]. The calculated equilibrium volumes of the three crystals are close to the measured volumes with a slight overestimation for GGG. GGG also has a smaller bulk modulus than the other three crystals. The calculated density of states and their atomic and orbital decompositions are presented and contrasted. All four crystals show very similar band structures and interatomic bonding. However, it is found that in GSGG and GSAG crystals, the Sc atom at the octahedral site shows a higher covalent character and an increased bond order in comparison to Ga or Al at the same site. This result may provide some insight into the significant difference in the radiation hardness of $\text{Cr}^{3+}:\text{Nd}^{3+}:\text{GSGG}$ as compared to $\text{Nd}^{3+}:\text{YAG}$.

I. INTRODUCTION

The synthetic inorganic compounds with a garnet structure have many interesting properties.¹ The best known is yttrium aluminum garnet ($\text{Y}_3\text{Al}_5\text{O}_{12}$) or YAG and yttrium iron garnet ($\text{Y}_3\text{Fe}_5\text{O}_{12}$) or YIG. The former is an important laser host material and the latter is a ferrimagnetic crystal important in microwave applications. The general garnet crystal of chemical formula $A_3B'_2B''_3\text{O}_{12}$ has a space group of $Ia\bar{3}d$. The cubic cell contains eight formula units where the metal ions A, B', B'' occupy the $24(c)$, $16(a)$, and $24(d)$ sites, respectively, and the O ions occupy the $96(h)$ sites. The garnet structure can be viewed as interconnected dodecahedrons (at the A site), octahedrons (at the B' site), and tetrahedrons (at the B'' site) with shared O atoms at the corners of the polyhedra.² Each O is a member of two dodecahedra, one octahedron, and one tetrahedron. The A site is usually occupied by a rare-earth ion and the B' and B'' by transition elements such as Fe or Sc, or metalloid elements such as Al or Ga. It is possible to have the B' and B'' sites occupied by the same element in different valence states such as in YAG, YIG, and or gadolinium gallium garnet ($\text{Gd}_3\text{Ga}_5\text{O}_{12}$) or GGG.

There are three main classes of synthetic garnets based on the atomic species at the B'' sites. They are aluminum garnets, iron garnet, and gallium garnets.¹ Similar to YAG, the gallium garnets are also important host materials for laser technology and are often used as substrate materials for film growth. Among them, $\text{Gd}_3\text{Sc}_2\text{Ga}_3\text{O}_{12}$ (GSGG), $\text{Gd}_3\text{Sc}_2\text{Al}_3\text{O}_{12}$ (GSAG), and $\text{Gd}_3\text{Ga}_5\text{O}_{12}$ (GGG) are the most common. In particular, GSGG and GSAG, when doped with Cr^{3+} and Nd^{3+} ions, have been shown to be promising host materials for the tunable infrared lasers.³⁻⁵ Tetravalent Cr^{4+} ions at the B'' sites in garnet crystals are promising materials for saturable absorbers in the near-infrared region.⁶ Amor-

phization of garnet crystals by applying high pressure⁷ or by neutron irradiation⁸ have been reported. In the later case, thermoannealing can restore the crystalline phase. Site exchange between metal ions at different sites is one of the most common types of defects in garnet crystals. The possibility of a noncubic symmetry in garnet crystals due to site exchange of the metal ions was raised based on the extended x-ray-absorption fine-structure (EXAFS) spectral measurement.⁹

It has also been reported that GSGG laser crystals are more resistant to radiation than YAG laser crystals when exposed to ionizing radiation,¹⁰ thus GSGG is potentially more suitable for laser applications in a hostile environment. Little is known about the source of the radiation hardness in GSGG in comparison with YAG. Could it be due to the intrinsic properties of the bulk crystal, or does it have to do with the impurity levels of the doped ions in the particular crystal? What are the relationships of various ions in the garnet structure to its physical and mechanical properties? To answer these questions, a fundamental understanding of the electronic structure and bonding in garnet crystals is necessary.

Radiation effects in crystalline solids have been a topic of research for many years, with most early work being performed on the alkali-halide crystals. As solid-state materials became viable as laser sources experimental research expanded to include these crystals as well. However, theoretical analysis did not proceed as quickly primarily due to the complexity of typical laser hosts. Theoretical studies concerning the radiation effects on laser crystals are scant even at this time. Evidence of laser performance degradation caused by irradiation with high-energy photons, electrons, and γ rays was observed in $\text{Nd}:\text{YAG}$ in the form of an increase in the optical threshold and a decrease in the optical efficiency.^{11,12} These effects have been attributed to the production of an additional optical loss within the material,

which has been associated with color centers introduced by irradiation.¹¹ Similar results were observed in ruby lasers (Cr:Al₂O₃) with an important exception that the laser exhibited increased optical efficiency when irradiated under strong pumping.¹³ The threshold behavior in ruby was attributed to color-center production as well, while the increased efficiency was attributed to absorption of the incident radiation by the Cr³⁺ ions. The same threshold effect in crystals with different dopant ions is evidence that bulk-crystal properties play a nontrivial role in determining the radiation hardness of a solid-state laser material.

GSGG laser crystals were first introduced in the early 1980s, with Cr:Nd:GSGG emerging as a common solid-state laser crystal several years later. This crystal is more efficient under pulsed, flashlamp pumping than Nd:YAG due to the broad absorption bands of the Cr³⁺ ion and the highly efficient transfer of energy from the Cr³⁺ ion to the Nd³⁺ ion, which is responsible for the lasing action.¹⁴ This increased efficiency makes Cr:Nd:GSGG an attractive alternative to Nd:YAG for certain applications, including weapon components and space applications. To that end the effects of ionizing radiation on Cr:Nd:GSGG were measured and compared to the effects in Nd:YAG. The GSGG-based laser did not show any evidence of performance change under irradiation.¹⁰ A more detailed experiment that included transient effects demonstrated the gain increase attributed to radiation pumping of the Cr³⁺ ion along with the radiation hardness of a laser utilizing Cr:Nd:GSGG.¹⁵ The evidence thus seems to indicate that color-center formation is less efficient in the GSGG crystal than in the YAG crystal and that this phenomena is, at least in part, a mechanism inherent to the bulk-crystal host rather than the dopant impurity ions.

There have been no *ab initio* calculations of the electronic structure of the garnet crystal until recently.¹⁶ This is mainly due to the considerable complexity of the crystal structure that posts a severe challenge to most *ab initio* electronic structure methods. We have recently used the density-functional-theory-based orthogonalized linear combinations of atomic orbitals (OLCAO) method to obtain the band structure of YAG.¹⁶ The nature of atomic bonding in the Y-Al-O system as a whole was also studied in considerable detail.¹⁷ Even more recently, the impurity levels of Cr³⁺ and Cr⁴⁺ ions in YAG and the related excited-state absorption were studied for the first time.¹⁸ In this paper, we employ the same method to investigate the electronic structure and bonding in three gallium garnets, GSGG, GSAG, and GGG, and compare them with the results of the YAG crystal. No previous calculations of the electronic structures on these garnet crystals are available. In the next section, we briefly outline our method of calculation. The main results of our investigation are presented and discussed in Sec. III. Section IV uses these results to present a conceptual analysis of the differing radiation-hardness properties of Nd:YAG and Cr:Nd:GSGG. Some conclusions are presented in the last section.

II. METHOD OF CALCULATION

We used the *ab initio* OLCAO method for the present calculation.¹⁶ The method has been described well before¹⁹ and will not be repeated. A full basis expansion consisting of

TABLE I. Atomic orbitals used for the basis expansion in the present calculation.

Atom	Core orbitals	Valence orbitals	Extra orbitals
Y	Krypton core	5s,4p,4d	6s,5p,5d
Gd	Xenon core	6s,6p,5d	
Sc	Argon core	4s,4p,3d	5s,4d
Ga	Argon core	4s,4p,3d	5s,5p,4d
Al	Neon core	3s,3p	4s,4p,3d
O	1s core	2s,2p	3s,3p

atomic orbitals was used which are listed in Table I. The semicore states of Gd 5p, Sc 3p, and Ga 3d were treated as valence states since their orbital energies are not very deep. The core states were orthogonalized to the noncore states and later eliminated from the secular equation.¹⁹ The 4f orbitals of Gd were not included since they have a closed-shell structure and are very localized with virtually no interaction with other orbitals. The actual 4f states in the Gd-related garnet crystals are more like deep core states and can be ignored. The computational procedures, the *k* points used, and other details are exactly the same as in the YAG crystal.¹⁶ Experimental lattice constants were used for calculations of GSGG (Ref. 20), GSAG (Ref. 20), GGG (Ref. 21), and YAG (Ref. 22) crystals. They are listed in Table II. For bulk properties, the total energies (TE's) of the garnet crystals were calculated as a function of crystal volume with the internal parameters fixed. For effective charges on each atom and bond order between a pair of atoms, separate calculations using a minimal basis were carried out. A minimal basis set consists of the valence orbitals listed in Table I. For that purpose, Al 3d was included in the minimal basis.

III. RESULTS

A. Bulk properties

The calculated TE data as a function of crystal volume for the three crystals were fitted to the Murnaghan equation of state (EOS).²³ The predicted values of equilibrium constant, bulk modulus *B*, and pressure coefficient *B'* are listed in Table II together with the results for YAG.¹⁶ The use of other forms of EOS such as the Birch-Murnaghan EOS (Ref. 24) or fourth-order polynomial fit results in a very minor difference in *B* but up to 10–15% difference in *B'*. The calculated lattice constants are very close to the measured ones except for the GGG crystal, where the lattice constant

TABLE II. Crystal parameters and calculated properties of the four garnet crystals.

Crystals	GSGG	GSAG	GGG	YAG
<i>a</i> (Å)	12.558 8	12.388 8	12.3829	12.000
<i>x</i>	−0.028 97	−0.032 16	−0.0280	−0.0306
<i>y</i>	0.056 98	0.054 93	0.0539	0.0512
<i>z</i>	0.153 47	0.155 66	0.1502	0.1500
<i>E_g</i> (eV)	4.21	4.88	4.03	4.71
O 2p bandwidth	5.92	5.34	6.85	6.47
O 2s bandwidth	1.22	1.60	1.43	2.01

TABLE III. Calculated bulk modulus and pressure coefficient of the garnet crystals.

	GSGG	GSAG	GGG	YAG
a/a_0	1.000	0.995	1.027	0.990
B	168.3	191.6	122.9	220.7
Expt.				220, ^a 185, ^b 189 ^c
B'	5.42	4.54	5.11	4.12

^aReference 25.

^bReference 26.

^cReference 27.

was overestimated by 2.7%. This is a somewhat larger discrepancy than what usually can be obtained by the OLCAO–local-density approximation (LDA) method. One possible reason for the larger discrepancy is that the potential function representation used for the Ga atom at two different sites was not sufficiently optimized for high precision. Nevertheless, we do not expect the electronic structure result to be much affected since it was calculated using the experimental lattice constants.

According to the results listed in Table III, YAG has the highest bulk modulus and GGG the smallest. Those of GSAG and GSGG are intermediate. The calculated value of $B=122.9$ GPa for GGG appears to be low and has to be treated with caution. Our past experience indicates that a crystal with overestimated lattice constants tends to have a lower bulk modulus. Experimental values of B are available only for YAG,^{25–27} which are listed in Table III and are in good agreement with the calculation.

B. Band structure and density of states

Figure 1 shows the calculated band structures of GSGG, GSAG, and GGG crystals. That of YAG can be found in Ref. 16. All four crystals have a direct band gap at Γ and very similar band structures. All three crystals have a single band at the bottom of the conduction band (CB) and the very flat top of the valence band (VB). This is in contrast to the case in YAG, where there are two bands dipping down at Γ .¹⁶ The s electrons of the rare-earth element mostly determine the CB minimum in a garnet crystal. This difference simply reflects the difference in the Gd-O and Y-O interactions. The values of the band gap and the widths of the O VB's are listed in Table II. GSAG (GGG) has the largest (smallest) calculated band gap of 4.88 eV (4.03 eV). It should be noted that calculated band gap of an insulator using the LDA

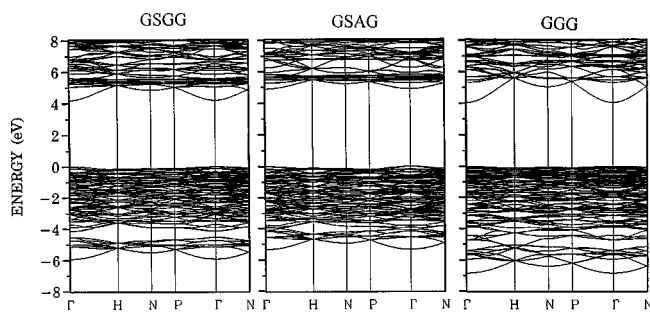


FIG. 1. Calculated band structures of (a) GSGG, (b) GSAG, and (c) GGG.

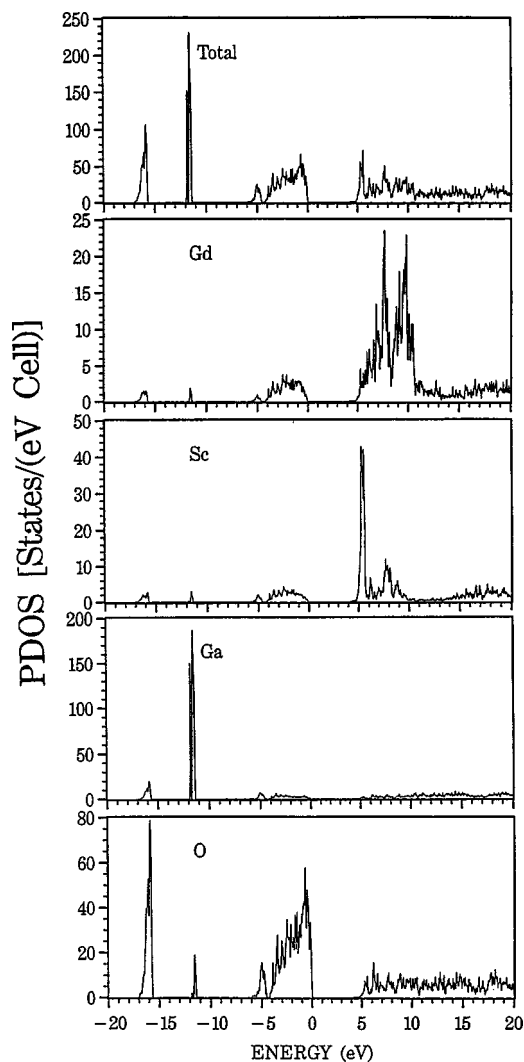


FIG. 2. Calculated total DOS and atom-resolved PDOS of GSGG: (a) total, (b) Gd, (c) Sc, (d) Ga, and (e) O.

theory is generally underestimated by about 25–30% from the experimental data. Only the YAG crystal has a reported experimental gap value of about 6.5 eV deduced from optical measurement.^{28,29} We are not aware of other measurements for the band gap in GSGG, GSAG, or GGG crystals.

The total and atom-resolved partial density of states (PDOS) in GSGG, GSAG, and GGG crystals are shown in Figs. 2, 3, and 4, respectively. The sharp peaks at near -11.7 eV in GSGG and GGG come from the localized semicore levels of the Ga $3d$ orbital, which were treated as valence states. The VB DOS consists mainly of an upper O $2p$ band and a lower O $2s$ band. The structures and the widths of these bands are only slightly different among the four crystals, reflecting minor differences in cation-O interactions. From Table II, it can be seen that GGG (GSAG) has the largest (smallest) O $2p$ bandwidth. For the O $2s$ band, YAG (GSGG) has the largest (smallest) width. The O $2p$ PDOS of the Gd-based garnets is very similar but differs significantly from that in YAG. This must be traced to the difference in the Al-O interaction and that of Ga-O or Sc-O interactions.

The orbital-resolved PDOS in the CB is important because it can be used to interpret the electron-loss near-edge spectra (ELNES) from the transmission electron microscope

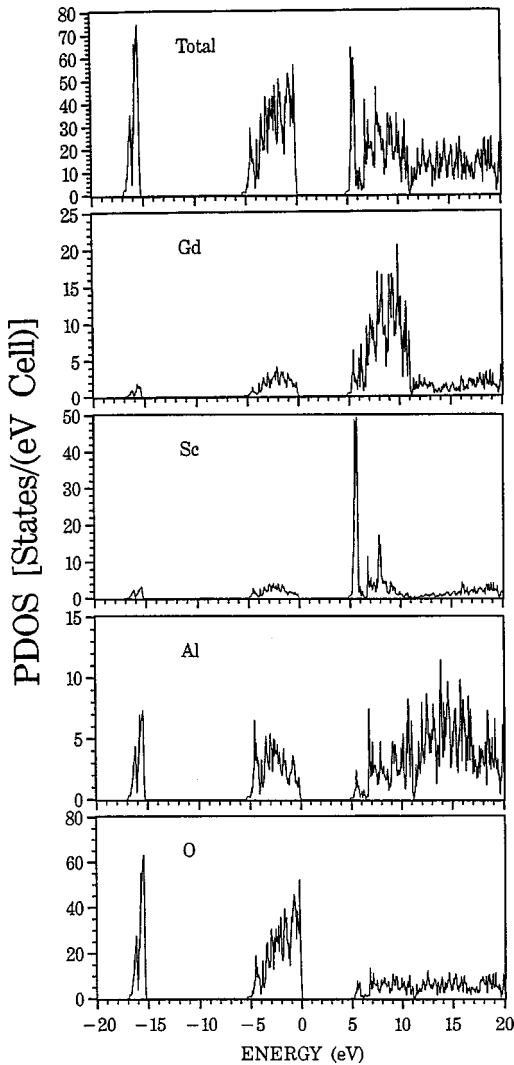


FIG. 3. Calculated total DOS and atom-resolved PDOS of GSAG: (a) total, (b) Gd, (c) Sc, (d) Al, and (e) O.

(TEM).³⁰ ELNES spectroscopy has become a very popular tool to investigate the local chemical and structural environment of a particular ion in a crystal. Within the dipole approximation, the $s+d$ component of the PDOS of the metal ions in the CB should mimic $L_{2,3}$ or $M_{2,3}$ edges (transitions from $2p$ or $3p$ core levels), and the p component of the PDOS the K edges (transitions from the $1s$ core level).³⁰ The CB PDOS generally shows more structures than the VB PDOS. The orbital-resolved PDOS (broadened by 1.0 eV) for the CB in GSGG, GSAG, and GGG is shown in Figs. 5, 6, and 7, respectively. These should be compared with the same for the YAG in Ref. 16. The following features are observed: (1) The Gd and Y PDOS's are dominated by the $5d$ or $4d$ states and have a split double peak. This splitting is less obvious in GSAG. (2) The width of the Gd $5d$ peaks in Ga garnets is wider than the Y $4d$ peak in YAG. (3) The PDOS's of Sc in GSGG and GSAG are almost identical and are dominated by a double-peak structure originated from Sc $3d$. This peak is at the CB edge and should be very easy to detect. (4) In GGG, the PDOS's of Ga at the octahedral site (Ga1) and the tetrahedral site (Ga2) are quite different. This is similar to Al at the two different sites in the YAG.¹⁶ (5) The PDOS's for Ga at the tetrahedral site (B'') in the three

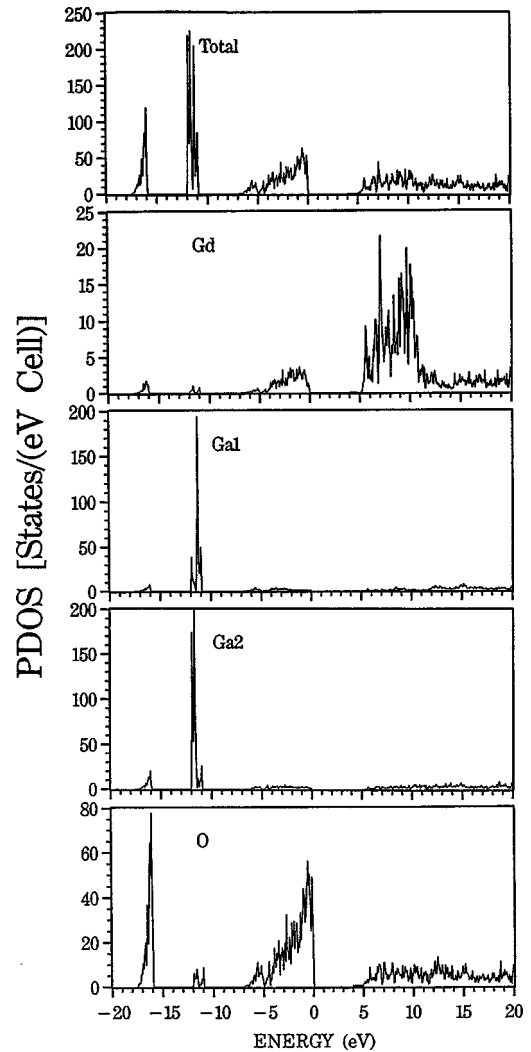


FIG. 4. Calculated total DOS and atom-resolved PDOS of GGG: (a) total, (b) Gd, (c) Ga1 (octahedral site), (d) Ga2 (tetrahedral site), and (e) O.

crystals are similar but with minor differences, indicating the sensitivity of the ELNES spectra to the local bonding environment. The amplitude of the $s+d$ component of Ga at the B'' site in GSAG is larger than its counterparts in GSGG and GGG. The CB PDOS for the YAG crystal is found to be in reasonable agreement with the measured ELNES spectra in YAG.³¹ No similar measurements for GSGG, GSAG, or GGG are available for comparison.

C. Effective charge and bond order

Based on separate minimal basis calculations using the Mulliken scheme,³² the effective charges Q^* and the bond order ρ_{ij} in the four crystals are listed in Tables IV and V, respectively. Although no large variations of Q^* among the four garnet crystals are expected, it is still worthwhile to note that the effective charge results show the GSGG crystal has a smaller charge transfer to the O ions and therefore is slightly less ionic. In particular, we note that at the octahedral B' site, Sc in GSGG and GSAG has a much larger effective charge than Al or Ga in YAG or GGG.

The bond order or the overlap population is a simple qualitative measure of the strength of the bond between a

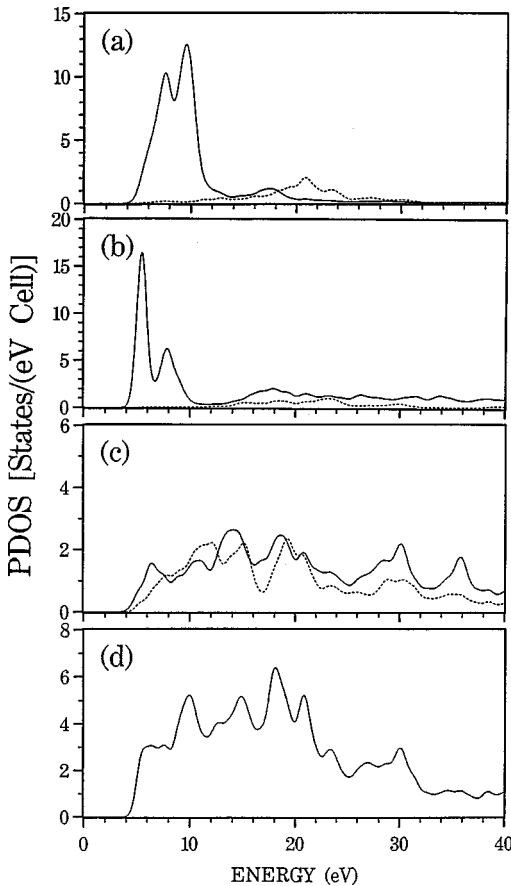


FIG. 5. Orbital-resolved PDOS in the empty CB in GSGG: (a) Gd, (b) Sc (c) Ga, and (d) O p component. In (a), (b), and (c), solid lines are for the $s+d$ components and dashed lines for the p components.

pair of atoms. In Table V, the calculated bond orders between metal ions and O in the four garnet crystals are listed together with the interatomic separations. The bond orders for the second-nearest-neighbor O-O pairs are also listed. As noted before, in YAG crystal, the bond order for Al(tet.)-O is relatively large compared to all other pairs.¹⁶ In the present case, we find that the bond order of 0.112 for Sc-O in GSGG is considerably larger than that of 0.096 for Al(oct.)-O in YAG, while the bond order of 0.121 for Ga-O in GSGG is slightly less than 0.133 for Al(tet.)-O in YAG. Thus the bond strength at the octahedral site in GSGG is stronger than that in YAG even though the bond length of 2.088 Å is actually longer than the corresponding distance in YAG. On the other hand, the bond order for the Gd-O pair is smaller than the Y-O pair in YAG. It is also noted that the bond orders for the O-O pairs in Ga garnets are larger than that in YAG mainly because of the shorter interatomic O-O separations.

In order to investigate in more detail the bonding difference in GSGG and YAG as demonstrated in the effective-charge and bond-order calculations, we display the valence charge-density distribution in two crystals on the (001) plane in Figs. 8(a) and 8(b). This plane contains all three types of cations. Also shown in Figs. 8(c) and 8(d) are the differences of the crystal charge and that of a superposition of neutral atomic charges on the same plane. The difference plots can illustrate the details of the charge transfer more clearly. The charge distribution and its relation to interatomic bonding in

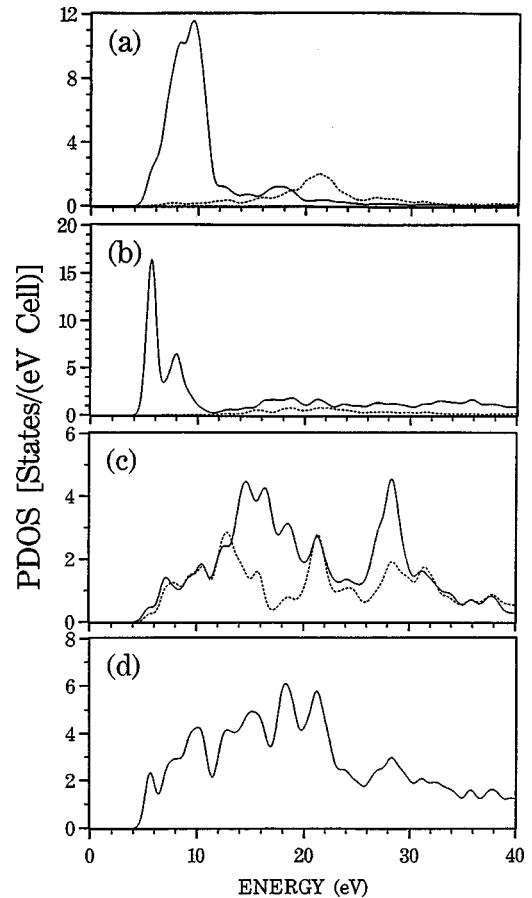


FIG. 6. Orbital-resolved PDOS in the empty CB in GSAG: (a) Gd, (b) Sc, (c) Al, and (d) O p component. In (a), (b), and (c), solid lines are for the $s+d$ components and dashed lines for the p components.

YAG have been discussed in considerable detail.¹⁶⁻¹⁸ As can be seen from Fig. 8, the Sc ion in GSGG has a much larger portion of the valence electron charge than Al in YAG. In Ref. 17, the possible interaction between Y and Al in YAG was pointed out based on the charge distribution between the two ions. The same cannot be said about Sc and Gd in GSGG. This difference in the charge distribution is even more pronounced in the difference plots shown in Figs. 8(c) and 8(d). There are more charges transferred from Al and Y to O in YAG than from Sc and Gd to O in GSGG.

IV. ANALYSIS OF RADIATION HARDNESS

The majority of the theoretical work concerning the effects of ionizing radiation in crystals has been performed using the alkali halides, as these are considered “typical” ionic compounds.³³ However, the general concepts developed for these crystals have been applicable to more complex materials such as those used for laser hosts.³⁴ In the generic alkali-halide structure the alkali-metal cation is surrounded by nearest-neighbor halogen anions. The more complicated garnet structures still emulate the alkali-halide model in the sense that the local neighborhood of the metal ion is that of a singular ion surrounded by nearest-neighbor ions of opposite charge. In the specific example of a YAG crystal yttrium is surrounded by eight nearest-neighbor oxy-

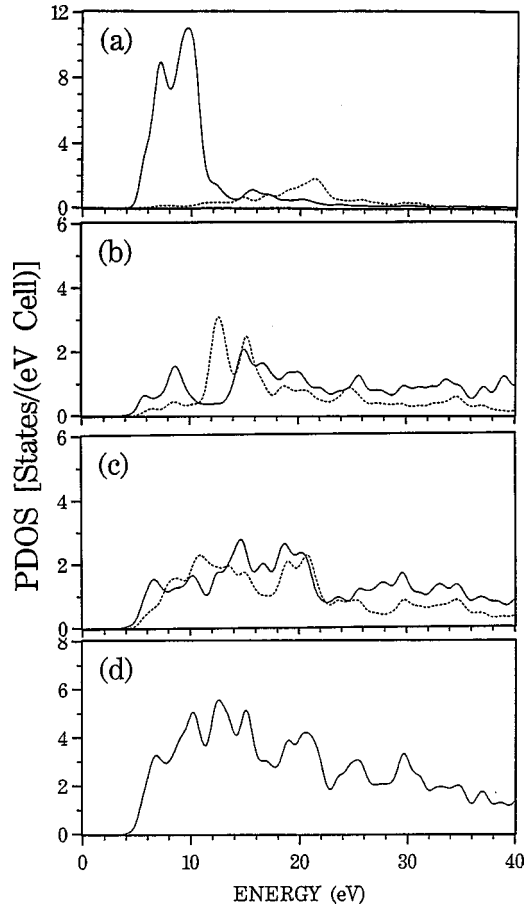


FIG. 7. Orbital-resolved PDOS in the empty CB in GGG: (a) Gd, (b) Ga (octahedral site), (c) Ga (tetrahedral site), and (d) O p component. In (a), (b), and (c), solid lines are for the $s+d$ components and dashed line for the p components.

gen ions, while aluminum is surrounded by either six (B') or four (B'') nearest-neighbor oxygen ions.¹⁶ For GSGG the gadolinium, scandium, and gallium are in the A , B' , and B'' sites as cations with oxygen as the anion. Therefore, within the alkali-halide approximation, it is the O bond with the individual cations that is of interest in studying the radiation hardness of these crystals.

TABLE IV. Calculated effective charge Q_{α}^* in the four garnet crystals.

	GSGG	GSAG	GGG	YAG
<i>A</i> site				
Y (exc. 4 <i>p</i>)				2.033
Gd (exc. 4 <i>f</i>)	1.895	1.903	1.424	
<i>B'</i> site				
Sc	2.291	2.276		
Al				1.939
Ga (exc. 3 <i>d</i>)			1.599	
<i>B''</i> site				
Al		1.893		1.839
Ga (exc. 3 <i>d</i>)	1.999		1.965	
<i>O</i> site				
O	6.645	6.672	6.748	6.708

TABLE V. Calculated bond order $\rho_{\alpha,\beta}$ in the four $A_3B_2B'_3O_{12}$ garnet crystals. Interatomic distances in parenthesis (\AA).

	GSGG	GSAG	GGG	YAG
<i>A</i> site				
Y-O				0.075 (2.432) 0.081 (2.303)
Gd-O	0.066 (2.477) 0.062 (2.392)	0.066 (2.479) 0.064 (2.371)	0.069 (2.473) 0.069 (2.358)	
<i>B'</i> site				
Sc-O	0.112 (2.088)	0.113 (2.083)		
Al-O				0.096 (1.937)
Ga-O			0.086 (2.006)	
<i>B''</i> site				
Al-O		0.132 (1.775)		0.133 (1.761)
Ga-O	0.121 (1.854)		0.121 (1.848)	
<i>O</i> site				
O-O	0.011 (2.815) 0.005 (2.808) 0.006 (2.808)	0.014 (2.705) 0.006 (2.815) 0.004 (2.852)	0.011 (2.808) 0.013 (2.705) 0.006 (2.848)	0.014 (2.658) 0.014 (2.696) 0.007 (2.837)

The effects of ionizing radiation in ionic crystals at room temperature are largely dominated by the formation of F and H centers, or rather, Frenkel pairs.³³ These defects are color centers formed by the displacement of an anion into an interstitial site as a result of electrons released by interaction

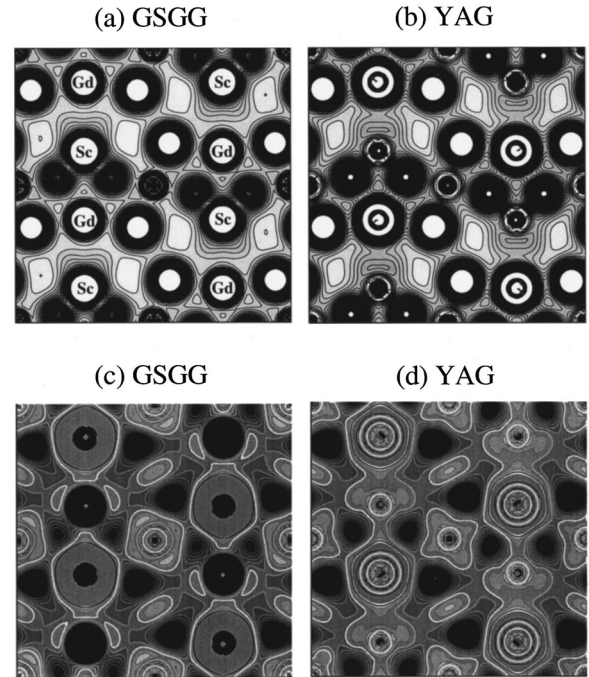


FIG. 8. Valence charge-density contours in the (001) plane containing all cations in (a) GSGG and (b) YAG. The positions of Gd and Sc are as marked. The Ga atoms are at the center and the corners of the plane. The O atoms are slightly above and below the plane. The contour lines range from 0.00 to 0.25 electrons/a.u.³ in intervals of 0.005. (c) and (d) show the difference between the crystal valence charge density and a superposition of atomic valence charges for GSGG and YAG on the same plane. The dark area represents a positive charge difference, the gray area negative charge difference, and the white area the zero charge difference.

with the incident radiation. The interstitial becomes the H center, while the vacancy generated from the absence of the anion traps free electrons to form the F center. A comparison of the individual oxygen bonds between YAG and GSGG can provide some insight into each crystal's susceptibility to forming these defects. Additionally, it has been demonstrated in alkali halides that a crystal is more susceptible to this type of coloration if the space between two adjacent halide ions (anions) is greater than half the atomic diameter of the associated halogen atom.³³ Furthermore, crystals with lower lattice energies have been observed to be more susceptible to color-center formation at room temperature as well.³⁵ The interatomic O spacing in YAG is slightly larger than the spacing in GSGG. However, in all of these garnet structures this distance is significantly larger than the atomic diameter of O, and it is therefore unlikely that this could be responsible for the difference between these two crystals. The bond order for the individual cation-O bonds are comparable for both crystals, with the exception of the B' site (Sc-O in GSGG and Al-O in YAG), which is larger for GSGG than for YAG. Since the bond order is a measure of the strength of the atomic bond, the larger value in GSGG implies a lesser susceptibility to defect formation. This viewpoint is consistent with radiation effects observed in ruby. Electronic structure calculation shows that the Al-O bond order in bulk ruby is comparable to that of YAG,^{17,36} and they have similar coloring when irradiated with ionizing radiation. If the bond order for the B' site is indeed indicative of the resistance of a crystal to radiation-induced defects, then GSAG should demonstrate the same characteristic radiation hardness as GSGG due to a similar bond order for this site. Radiation hardness, even in simple crystals, is a very complex issue. The above simple argument is admittedly speculative. More in-depth analysis requires additional experimental and theoretical work in future.

V. CONCLUSIONS

We have studied the electronic structure and bonding in several Ga garnet crystals and compared with that of YAG. We find that in general, the electronic structures in all garnet crystals are very similar. This is consistent with the fact that optical transitions of the same Mn^{3+} ion in different garnet crystals show similar emission spectra with only small shifts in peak positions.³⁷ However, small differences in interatomic bonding at different symmetry sites and with different cations can be documented. In particular, we find that the Sc ion at the octahedral site in GSGG and GSAG crystals has stronger bonds as reflected by their larger bond-order values in spite of larger interatomic separations. There is also less charge transfer from cations to O in GSGG and therefore a slightly higher covalent character. This may be related to the fact that a Cr^{3+} ion in GSGG crystal, which substitutes Sc at the octahedral site, is particularly stable and resistant to radiation. An approximation to the simpler alkali-halide ionic crystal is presented and used as a basis for presenting an analysis of the radiation hardness of these garnet crystals. While more persuasive argument must wait for detailed calculations involving substituted ions in the garnet crystal and the associated defect structures caused by radiation, the present study on the structure and bonding in the perfect bulk crystals is a first step towards this direction. It is also hoped that additional experimental measurements on high-quality single crystals will be performed. Experimental data, together with theoretical calculations, will provide a deeper understanding about the properties of various garnet crystals.

ACKNOWLEDGMENT

The work at UMKC was supported in part by the U.S. Department of Energy under Grant No. DE-FG02-84DR45170 and work at AS-FM&T was supported by Contract No. DE-AC04-76-DP00613.

*Author to whom correspondence should be addressed. Electronic address: chingw@umkc.edu

¹Franklin F. Y. Wang, in *Treatise of Materials Science and Technology*, edited by Herbert Herman (Academic Press, New York, 1973), pp. 279–384.

²F. S. Galasso, *Structure and Properties of Inorganic Solids* (Pergamon, New York, 1970), p. 244.

³L. J. Andrew, in *Tunable Solid-State Laser II*, edited by A. B. Budgor, L. Esterowitz, and L. G. DeShazer, (Springer-Verlag, New York, 1986), p. 44.

⁴B. Sturuve and G. Huber, *J. Appl. Phys.* **57**, 45 (1985).

⁵E. Reed, *IEEE J. Quantum Electron.* **QE-21**, 1625 (1985).

⁶A. Brignon and J.-P. Huignard, *Opt. Commun.* **110**, 717 (1994).

⁷H. Hua, J. Liu and Y. K. Vohra, *J. Phys.: Condens. Matter* **8**, L139 (1996).

⁸Yu. G. Chukalkin and V. R. Shtirts, *Phys. Status Solidi A* **144**, 9 (1994).

⁹Jun Dong and K. Lu, *Phys. Rev. B* **43**, 8808 (1991).

¹⁰E. V. Zharikov, I. I. Kuratev, V. V. Laptev, S. P. Nasel'skii, A. I. Ryabov, G. N. Toropkin, A. V. Shestakov, and I. A. Shcherbakov, *Seriya Fizicheskaya* **48**, 103 (1984).

¹¹D. M. J. Compton and R. A. Cesena, *IEEE Trans. Nucl. Sci.* **NS-14**, 55 (1967).

¹²J. A. Holzer and B. C. Passenheim, *Opt. Eng. (Bellingham)* **18**, 562 (1979).

¹³V. R. Johnson and R. W. Grow, *IEEE J. Quantum Electron.* **QE-3**, 1 (1967).

¹⁴D. Pruss, G. Huber, A. Beimowski, V. V. Laptev, L. A. Shcherbakov, and Y. V. Zharikov, *Appl. Phys. B* **28**, 355 (1982).

¹⁵P. J. Brannon; Sandia Report No. SAND94-2731, 1994 (unpublished).

¹⁶Y.-N. Xu and W. Y. Ching, *Phys. Rev. B* **59**, 10 530 (1999).

¹⁷W. Y. Ching and Y.-N. Xu, *Phys. Rev. B* **59**, 12 815 (1999).

¹⁸W. Y. Ching, Y.-N. Xu, and B. K. Brickeen, *Appl. Phys. Lett.* **74**, 3755 (1999).

¹⁹W. Y. Ching, *J. Am. Ceram. Soc.* **71**, 3135 (1990).

²⁰S. Yamazaki, F. Marumo, K. Tanaka, H. Morikawa, N. Kodama, K. Kitamura, and Y. Miyazawa, *J. Solid State Chem.* **108**, 94 (1994).

²¹J. Sasvari and P.-E. Werner, *Acta Chem. Scand.* **37**, 203 (1983).

²²F. Euler and J. A. Bruce, *Acta Crystallogr.* **19**, 971 (1965).

²³F. D. Murnagan, *Proc. Natl. Acad. Sci. USA* **30**, 244 (1944).

²⁴F. Birch, *J. Geophys. Res.* **83**, 1257 (1978).

²⁵A. M. Hofmeiser and K. R. Campbell, *J. Appl. Phys.* **72**, 638–646 (1992).

²⁶P. R. Stoddart, P. E. Ngoepe, P. M. Mjwara, J. D. Comins, and G. A. Saunders, *J. Appl. Phys.* **73**, 7298 (1993).

²⁷W. J. Alton and A. J. Barow, *J. Appl. Phys.* **32**, 1172 (1967).

²⁸Y. Zhan and P. D. Coleman, *Appl. Opt.* **23**, 548 (1984).

- ²⁹T. Tomiki, Y. Ganaha, T. Shikenbrau, T. Futemma, M. Yuri, Y. Aiura, H. Fukutani, H. Kato, J. Tamashiro, T. Miyahara, and A. Yonesu, *J. Phys. Soc. Jpn.* **62**, 1388 (1993); **65**, 1106 (1996).
- ³⁰R. F. Egerton, *Electron Energy Loss Spectroscopy in the Electron Microscopy* (Plenum, New York, 1993).
- ³¹M. A. Gülgün, W. Y. Ching, Y.-N. Xu, and M. Rühle, *Philos. Mag. B* **79**, 921 (1999).
- ³²R. S. Mulliken, *J. Chem. Phys.* **23**, 1833 (1955).
- ³³J. H. Schulman and W. D. Compton, *Color Centers in Solids* (Pergamon, New York, 1962).
- ³⁴Y. Farge and M. P. Fontana, *Electronic and Vibrational Properties of Point Defects in Ionic Crystals* (North-Holland, New York, 1979).
- ³⁵B. V. Budylin and A. A. Vorob'ev, *Effect of Radiation on Ionic Structures* (IPST, Jerusalem, 1964).
- ³⁶W. Y. Ching, Y. N. Xu, and M. Rühle, *J. Am. Ceram. Soc.* **80**, 3199 (1997).
- ³⁷S. Kück, S. Hartung, S. Harling, K. Determan, and G. Huber, *Phys. Rev. B* **57**, 2203 (1998).